Supplementary Information for *Single-ion 4f element magnetism: an ab-initio look at Ln(COT)$_2^-$*

Frédéric Gendron,[a] Benjamin Pritchard,[a] Hélène Bolvin,[b] and Jochen Autschbach* [a]

[a] Department of Chemistry, University at Buffalo,
State University of New York, Buffalo, NY 14260-3000, USA

[b] Laboratoire de Physique et de Chimie Quantique,
Université Toulouse 3, 31062 Toulouse, France

email: bolvin@irsamc.ups-tlse.fr, jochena@buffalo.edu

Contents:

Optimized Distances of $Ln(COT)_2^-$

Table S1: Comparison of selected optimized distances (Å) along the $Ln(COT)_2^-$ series. SF ZORA/B3LYP/TZ2P. Fractional occupation $(4f_\sigma 4f_\pi 4f_\delta 4f_\phi)^n$.

Complex	Ln–COT	Ln–C	C–C
$Ce(COT)_2^-$	2.133	2.817	1.408
$Pr(COT)_2^-$	2.123	2.809	1.408
$Nd(COT)_2^-$	2.131	2.815	1.408
$Pm(COT)_2^-$	2.156	2.834	1.408
$Sm(COT)_2^-$	2.156	2.834	1.408
$Eu(COT)_2^-$	2.101	2.793	1.408
$Gd(COT)_2^-$	2.023	2.734	1.408
$Tb(COT)_2^-$	2.004	2.721	1.408
$Dy(COT)_2^-$	1.999	2.716	1.408
$Ho(COT)_2^-$	2.009	2.724	1.408
$Er(COT)_2^-$	2.032	2.741	1.408
$Tm(COT)_2^-$	2.030	2.740	1.408
$Yb(COT)_2^-$	1.981	2.704	1.408

Table S2: $Ce(COT)_2^-$: Principal optimized distances (Å) and relative energies (cm^{-1}) of the SF and SO states using three different fractional occupation schemes[a].

	Frac17	Frac13	NoFrac
Ce–COT	2.133	2.134	2.141
Ce–C	2.817	2.817	2.822
C–C	1.408	1.408	1.408
		Spin-Free ^2F term	
$^2\Sigma$	0	0	0
$^2\Pi$	518	518	518
$^2\Phi$	621	621	612
$^2\Delta$	1917	1917	1897
		Spin-Orbit $^2F_{5/2}$ term	
±1/2	0	0	0
±5/2	479	480	469
±3/2	1040	1040	1032

[a] Frac17: $(4f_\sigma 4f_\pi 4f_\delta 4f_\phi)^1$ Frac13: $(4f_\sigma 4f_\pi)^1$ NoFrac: $4f_\sigma^1$

Model vs. *ab-initio* for $Ce(COT)_2^-$ and $Pr(COT)_2^-$

Table S3: Model wave functions[i] $\vert\psi\rangle$, orbital $m_u^L(\boldsymbol{r})$ and spin $m_u^S(\boldsymbol{r})$ magnetizations for $Ce(COT)_2^-$ and $Pr(COT)_2^-$.

	$Ce(COT)_2^-$		
ψ	$= A\,^2\Sigma_{1/2} - B\,^2\Pi_{1/2}\ \ (u = \Vert)$	ψ	$= \frac{1}{\sqrt{2}}\left[A\,^2\Sigma_{1/2} - B\,^2\Pi_{1/2} + A\,^2\Sigma_{-1/2} - B\,^2\Pi_{-1/2}\right]\ \ (u = \perp)$
	$= AY_3^0 - B\bar{Y}_3^1$	ψ	$= \frac{1}{\sqrt{2}}\left[AY_3^0 - B\bar{Y}_3^1 + A\bar{Y}_3^0 - BY_3^{-1}\right]$
$m_\Vert^S(\boldsymbol{r})$	$= \frac{1}{2}\left[A^2Y_3^0Y_3^0 + B^2Y_3^1Y_3^{-1}\right]$	$m_\perp^S(\boldsymbol{r})$	$= \frac{A^2}{2}\left[Y_3^0Y_3^0\right] - \frac{B^2}{4}\left[Y_3^1Y_3^1 + Y_3^{-1}Y_3^{-1}\right]$
	$= \frac{A^2}{2}f_0^2 - \frac{B^2}{4}\left[f_{1+}^2 + f_{1-}^2\right]$		$= \frac{A^2}{2}f_0^2 - \frac{B^2}{4}\left[f_{1-}^2 - f_{1+}^2\right]$
$m_\Vert^L(\boldsymbol{r})$	$= -B^2Y_3^1Y_3^{-1}$	$m_\perp^L(\boldsymbol{r})$	$= -\frac{AB\sqrt{12}}{2}Y_3^0Y_3^0 + \frac{AB\sqrt{3}}{4}\left[2Y_3^1Y_3^{-1} + Y_3^1Y_3^1 + Y_3^{-1}Y_3^{-1}\right]$
	$= \frac{B^2}{2}\left[f_{1+}^2 + f_{1-}^2\right]$		$= -\frac{AB\sqrt{12}}{2}f_0^2 - AB\sqrt{3}f_{1+}^2$
	$Pr(COT)_2^-$		
ψ	$= A\,^3\Gamma_{-3} + B\,^3\Phi_{-3} + C\,^3\Delta_{-3}\ \ (u = \Vert)$		
	$= A\vert Y_3^{-3}Y_3^{-1}\vert + \frac{B}{\sqrt{2}}\left[\sqrt{\frac{2}{3}}(\vert Y_3^{-3}\bar{Y}_3^0\vert - \vert\bar{Y}_3^{-3}Y_3^0\vert) + \sqrt{\frac{1}{3}}(\vert Y_3^{-2}\bar{Y}_3^{-1}\vert - \vert\bar{Y}_3^{-2}Y_3^{-1}\vert)\right]$		
	$+C\left[\sqrt{\frac{2}{3}}\vert\bar{Y}_3^{-2}\bar{Y}_3^0\vert + \sqrt{\frac{1}{3}}\vert\bar{Y}_3^{-3}\bar{Y}_3^1\vert\right]$		
$m_\Vert^S(\boldsymbol{r})$	$= -\frac{A^2}{2}\left[Y_3^3Y_3^{-3} + Y_3^1Y_3^{-1}\right] - \frac{C^2}{3}\left[Y_3^2Y_3^{-2} + Y_3^0Y_3^0\right] + \frac{C^2}{6}\left[Y_3^3Y_3^{-3} + Y_3^1Y_3^{-1}\right]$		
	$= \frac{A^2}{4}\left[f_{3+}^2 + f_{3-}^2 + f_{1+}^2 + f_{1-}^2\right] - \frac{C^2}{6}\left[f_{2+}^2 + f_{2-}^2\right] - \frac{C^2}{3}f_0^2 - \frac{C^2}{6}\left[f_{3+}^2 + f_{3-}^2 + f_{1+}^2 + f_{1-}^2\right]$		
$m_\Vert^L(\boldsymbol{r})$	$= 2A^2\left[Y_3^3Y_3^{-3} + Y_3^1Y_3^{-1}\right] - \frac{3B^2}{2}\left[\frac{2}{3}[Y_3^0Y_3^0 - Y_3^3Y_3^{-3}] + \frac{1}{3}[Y_3^2Y_3^{-2} - Y_3^1Y_3^{-1}]\right]$		
	$-C^2\left[\frac{2}{3}[Y_3^2Y_3^{-2} + Y_3^0Y_3^0] - \frac{1}{3}[Y_3^3Y_3^{-3} + Y_3^1Y_3^{-1}]\right]$		
	$= -A^2\left[f_{3+}^2 + f_{3-}^2 + f_{1+}^2 + f_{1-}^2\right] - \frac{3B^2}{2}\left[\frac{2}{3}[f_0^2 + \frac{1}{2}(f_{3+}^2 + f_{3-}^2)] + \frac{1}{6}[f_{2+}^2 + f_{2-}^2 + f_{1+}^2 + f_{1-}^2]\right]$		
	$-C^2\left[\frac{2}{3}[f_0^2 + \frac{1}{2}(f_{2+}^2 + f_{2-}^2)] + \frac{1}{6}[f_{3+}^2 + f_{3-}^2 + f_{1+}^2 + f_{1-}^2]\right]$		

[i] Notation: Angular behavior only. Spherical harmonics $Y_\ell^{m_\ell}$, a bar indicates beta spin. Tesseral harmonics $f_{\ell\pm}^{|m|}$. Two-electron Slater determinants $|a, b| = 1/\sqrt{2}\,\det |a, b|$. Real coefficients A, B, C. Normalization implies $A^2 + B^2 = 1$ for $Ce(COT)_2^-$ and $A^2 + B^2 + C^2 = 1$ for $Pr(COT)_2^-$.

The spherical harmonics $Y_\ell^{m_\ell}$ are related to the real tesseral harmonics $f_{\ell\pm}^{|m|}$ as follows:

$$Y_3^0 = f_0$$
$$Y_3^1 = \frac{f_{1+} - if_{1-}}{i\sqrt{2}}$$
$$Y_3^{-1} = \frac{f_{1+} + if_{1-}}{i\sqrt{2}}$$
$$Y_3^2 = \frac{f_{2+} + if_{2-}}{\sqrt{2}}$$
$$Y_3^{-2} = \frac{f_{2+} - if_{2-}}{\sqrt{2}}$$

$$Y_3^3 = \frac{f_{3+} - i f_{3-}}{i\sqrt{2}}$$

$$Y_3^3 = \frac{f_{3+} + i f_{3-}}{i\sqrt{2}}$$

Table S4: Comparison of the orbital and spin expectation values obtained with the model and with the *ab-initio* calculations for $Ce(COT)_2^-$ and $Pr(COT)_2^-$.

	Model	*ab-initio*
	$Ce(COT)_2^-$	
$\langle L_\parallel \rangle$	0.459	0.461
$\langle S_\parallel \rangle$	0.040	0.038
$\pm g_\parallel$	1.078	1.074
$\langle L_\perp \rangle$	-1.726	-1.716
$\langle S_\perp \rangle$	0.269	0.269
$\pm g_\perp$	2.376	2.354
	$Pr(COT)_2^-$	
$\langle L_\parallel \rangle$	-3.578	-3.609
$\langle S_\parallel \rangle$	0.609	0.613
$\pm g_\parallel$	4.720	4.765

Energies and assignment of the lowest Spin-Free electronic states in $Ln(COT)_2^-$

Table S5: Relative energies (cm^{-1}) and assignment (per-cent) of the SF states issued from the SF ground multiplet ^{2s+1}L. CAS(n,7)SCF calculations.

^{2s+1}L Multiplet	M_L States[a]	ΔE	Major Configurations[b]
		$Ce(COT)_2^-$	
^2F	$^2\Sigma$	0	100 σ
	$^2\Pi$	518	100 π
	$^2\Phi$	621	100 ϕ
	$^2\Delta$	1917	100 δ
		$Pr(COT)_2^-$	
^3H	$^3\Phi$	0	76 ($\sigma\phi$), 22 ($\delta\pi$)
	$^3\Gamma$	4	93 ($\phi\pi$)
	$^3\Delta$	421	61 ($\sigma\delta$), 36 ($\phi\pi$)
	$^3\Sigma$	637	72 ($\pi\pi$), 26 ($\delta\delta$)
	$^3\Pi$	644	58 ($\pi\delta$), 28 ($\sigma\pi$)
	^3H	1298	100 ($\phi\delta$)
		$Nd(COT)_2^-$	
^4I	$^4\Phi$	0	76 ($\pi\pi\phi$), 15 ($\phi\delta\delta$), 8 ($\sigma\pi\delta$)
	$^4\Gamma$	28	51 ($\pi\phi\delta$), 48 ($\sigma\pi\phi$)
	$^4\Delta$	288	48 ($\pi\phi\delta$), 27 ($\sigma\pi\phi$), 26 ($\pi\pi\delta$)
	^4H	413	100 ($\sigma\phi\delta$)
	$^4\Pi$	606	39 ($\sigma\phi\delta$), 25 ($\pi\delta\delta$), 23 ($\sigma\pi\delta$), 12 ($\pi\phi\phi$)
	$^4\Sigma$	732	53 ($\sigma\delta\delta$), 22 ($\pi\phi\delta$), 19 ($\sigma\phi\phi$), 6 ($\sigma\pi\pi$)
	^4I	758	100 ($\pi\phi\delta$)
		$Pm(COT)_2^-$	
^5I	^5I	0	100 ($\sigma\pi\phi\delta$)
	$^5\Sigma$	26	57 ($\pi\pi\phi\phi$), 20 ($\sigma\pi\phi\delta$), 16 ($\pi\pi\delta\delta$), 5 ($\phi\phi\delta\delta$)
	$^5\Pi$	129	37 ($\pi\pi\phi\delta$), 28 ($\sigma\pi\phi\phi$), 20 ($\pi\phi\phi\delta$), 11 ($\sigma\pi\delta\delta$)
	^5H	319	100 ($\pi\pi\phi\delta$)
	$^5\Delta$	363	46 ($\sigma\pi\phi\delta$), 27 ($\sigma\phi\phi\delta$), 22 ($\pi\phi\delta\delta$)
	$^5\Phi$	560	69 ($\sigma\phi\delta\delta$), 21 ($\sigma\pi\pi\phi$), 9 ($\pi\phi\phi\delta$)
	$^5\Gamma$	577	54 ($\sigma\pi\phi\delta$), 42 ($\pi\phi\delta\delta$)
		$Sm(COT)_2^-$	
^6H	^6H	0	100 ($\sigma\pi\pi\phi\delta$)
	$^6\Sigma$	379	49 ($\sigma\phi\phi\delta\delta$), 47 ($\sigma\pi\pi\phi\phi$)
	$^6\Pi$	473	64 ($\sigma\pi\phi\phi\delta$), 20 ($\pi\phi\phi\delta\delta$), 15 ($\sigma\pi\pi\phi\delta$)
	$^6\Delta$	629	69 ($\pi\pi\phi\phi\delta$), 31 ($\sigma\pi\phi\delta\delta$)
	$^6\Phi$	802	60 ($\pi\pi\phi\delta\delta$), 40 ($\sigma\pi\phi\phi\delta$)
	$^6\Gamma$	861	100 ($\sigma\pi\phi\delta\delta$)
		$Eu(COT)_2^-$	
^7F	$^7\Delta$	0	100 ($\sigma\pi\pi\phi\phi\delta$)
	$^7\Phi$	525	100 ($\sigma\pi\pi\phi\delta\delta$)
	$^7\Pi$	871	100 ($\sigma\pi\phi\phi\delta\delta$)
	$^7\Sigma$	1102	100 ($\pi\pi\phi\phi\delta\delta$)

[a]: The SF states characterized by the total angular momentum projection $M_L = \sum m_\ell$ are denoted using the $D_\infty h$ parent symmetry. [b]: Numbers indicate the weight of the configurations in %, only contributions larger than 5% are listed.

Table S6: Relative energies (cm^{-1}) and assignment (per-cent) of the SF states issued from the SF ground multiplet ^{2s+1}L. CAS(n,7)SCF calculations.

^{2s+1}L Multiplet	M_L States[a]	ΔE	Major Configurations[b]
			$Gd(COT)_2^-$
^8S	$^8\Sigma$	0	100 $(\sigma\pi\pi\phi\phi\delta\delta)$
			$Tb(COT)_2^-$
^7F	$^7\Sigma$	0	100$(\sigma^2\pi^1\pi^1\phi^1\phi^1\delta^1\delta^1)$
	$^7\Pi$	268	100$(\sigma^1\pi^2\pi^1\phi^1\phi^1\delta^1\delta^1)$
	$^7\Phi$	675	100$(\sigma^1\pi^1\pi^1\phi^2\phi^1\delta^1\delta^1)$
	$^7\Delta$	1147	100$(\sigma^1\pi^1\pi^1\phi^2\phi^1\delta^1\delta^1)$
			$Dy(COT)_2^-$
^6H	$^6\Phi$	0	70 $(\sigma^2\pi^1\pi^1\phi^2\phi^1\delta^1\delta^1)$, 30 $(\sigma^1\pi^2\pi^1\phi^1\phi^1\delta^2\delta^1)$
	$^6\Gamma$	35	100 $(\sigma^1\pi^2\pi^1\phi^2\phi^1\delta^1\delta^1)$
	$^6\Delta$	152	65 $(\sigma^2\pi^1\pi^1\phi^1\phi^1\delta^2\delta^1)$, 34 $(\sigma^1\pi^2\pi^1\phi^2\phi^1\delta^1\delta^1)$
	$^6\Sigma$	217	66 $(\sigma^1\pi^2\pi^2\phi^1\phi^1\delta^1\delta^1)$, 31 $(\sigma^1\pi^1\pi^1\phi^1\phi^1\delta^2\delta^2)$
	$^6\Pi$	223	63 $(\sigma^1\pi^2\pi^1\phi^1\phi^1\delta^2\delta^1)$, 27 $(\sigma^2\pi^2\pi^1\phi^1\phi^1\delta^1\delta^1)$, 9 $(\sigma^2\pi^1\pi^1\phi^2\phi^1\delta^2\delta^1)$
	^6H	865	100 $(\sigma^1\pi^1\pi^1\phi^2\phi^1\delta^2\delta^1)$
			$Ho(COT)_2^-$
^5I	$^5\Phi$	0	75 $(\sigma^1\pi^2\pi^2\phi^2\phi^1\delta^1\delta^1)$, 16 $(\sigma^1\pi^1\pi^1\phi^2\phi^1\delta^2\delta^2)$, 9 $(\sigma^2\pi^1\pi^2\phi^1\phi^1\delta^2\delta^1)$
	$^5\Gamma$	33	53 $(\sigma^1\pi^2\pi^1\phi^2\phi^1\delta^2\delta^1)$, 47 $(\sigma^2\pi^2\pi^1\phi^2\phi^1\delta^1\delta^1)$
	$^5\Delta$	139	44 $(\sigma^1\pi^2\pi^1\phi^2\phi^1\delta^2\delta^1)$, 27 $(\sigma^1\pi^2\pi^2\phi^1\phi^1\delta^2\delta^1)$, 26 $(\sigma^2\pi^2\pi^1\phi^2\phi^1\delta^1\delta^1)$
	^5H	266	100 $(\sigma^2\pi^1\pi^1\phi^2\phi^1\delta^2\delta^1)$
	$^5\Pi$	303	38 $(\sigma^2\pi^1\pi^1\phi^2\phi^1\delta^2\delta^1)$, 26 $(\sigma^1\pi^1\pi^2\phi^1\phi^1\delta^2\delta^2)$, 23 $(\sigma^2\pi^2\pi^1\phi^1\phi^1\delta^2\delta^1)$
			12 $(\sigma^1\pi^2\pi^1\phi^2\phi^2\delta^1\delta^1)$
	$^5\Sigma$	373	55 $(\sigma^2\pi^1\pi^1\phi^1\phi^1\delta^2\delta^2)$, 21 $(\sigma^1\pi^2\pi^1\phi^2\phi^1\delta^2\delta^1)$, 18 $(\sigma^2\pi^1\pi^1\phi^2\phi^2\delta^1\delta^1)$
	^5I	484	100 $(\sigma^1\pi^2\pi^1\phi^2\phi^1\delta^2\delta^1)$
			$Er(COT)_2^-$
^4I	^4I	0	100 $(\sigma^2\pi^2\pi^1\phi^2\phi^1\delta^2\delta^1)$
	$^4\Sigma$	103	56 $(\sigma^1\pi^2\pi^2\phi^2\phi^2\delta^1\delta^1)$, 21 $(\sigma^2\pi^2\pi^1\phi^2\phi^1\delta^2\delta^1)$, 17 $(\sigma^1\pi^2\pi^2\phi^1\phi^1\delta^2\delta^2)$
			5 $(\sigma^1\pi^1\pi^1\phi^2\phi^2\delta^2\delta^2)$
	$^4\Pi$	163	37 $(\sigma^1\pi^2\pi^2\phi^2\phi^1\delta^2\delta^1)$, 28 $(\sigma^2\pi^2\pi^1\phi^2\phi^2\delta^2\delta^2)$, 12 $(\sigma^2\pi^2\pi^1\phi^1\phi^1\delta^2\delta^2)$
	^4H	196	100 $(\sigma^1\pi^2\pi^2\phi^2\phi^1\delta^2\delta^1)$
	$^4\Delta$	300	46 $(\sigma^2\pi^2\pi^1\phi^2\phi^1\delta^2\delta^1)$, 27 $(\sigma^2\pi^1\pi^1\phi^2\phi^2\delta^1\delta^2)$, 23 $(\sigma^1\pi^2\pi^1\phi^2\phi^1\delta^2\delta^2)$
	$^4\Gamma$	387	55 $(\sigma^2\pi^2\pi^1\phi^2\phi^1\delta^2\delta^1)$, 44 $(\sigma^1\pi^2\pi^1\phi^1\phi^2\delta^2\delta^2)$
	$^4\Phi$	408	71 $(\sigma^2\pi^1\pi^1\phi^2\phi^1\delta^2\delta^2)$, 20 $(\sigma^2\pi^2\pi^2\phi^2\phi^1\delta^2\delta^2)$, 9 $(\sigma^1\pi^2\pi^1\phi^2\phi^2\delta^2\delta^1)$
			$Tm(COT)_2^-$
^3H	^3H	0	100 $(\sigma^2\pi^2\pi^2\phi^1\phi^2\delta^1\delta^2)$
	$^3\Sigma$	500	53 $(\sigma^2\pi^1\pi^1\phi^2\phi^2\delta^2\delta^2)$, 43 $(\sigma^2\pi^2\pi^2\phi^2\phi^2\delta^1\delta^1)$
	$^3\Pi$	533	64 $(\sigma^2\pi^2\pi^1\phi^2\phi^2\delta^2\delta^1)$, 21 $(\sigma^1\pi^2\pi^1\phi^2\phi^2\delta^2\delta^2)$, 14 $(\sigma^2\pi^2\pi^2\phi^2\phi^1\delta^2\delta^1)$
	$^3\Delta$	592	67 $(\sigma^1\pi^2\pi^2\phi^2\phi^2\delta^2\delta^1)$, 33 $(\sigma^2\pi^2\pi^1\phi^2\phi^1\delta^2\delta^2)$
	$^3\Gamma$	615	100 $(\sigma^2\pi^2\pi^1\phi^2\phi^1\delta^2\delta^2)$
	$^3\Phi$	656	64 $(\sigma^1\pi^2\pi^2\phi^2\phi^1\delta^2\delta^2)$, 36 $(\sigma^2\pi^2\pi^1\phi^2\phi^2\delta^2\delta^1)$
			$Yb(COT)_2^-$
^2F	$^2\Delta$	0	100$(\sigma^2\pi^2\pi^2\phi^2\phi^2\delta^2\delta^1)$
	$^2\Phi$	182	100$(\sigma^2\pi^2\pi^2\phi^2\phi^1\delta^2\delta^2)$
	$^2\Pi$	643	100$(\sigma^2\pi^2\pi^1\phi^2\phi^2\delta^2\delta^2)$
	$^2\Sigma$	802	100$(\sigma^1\pi^2\pi^1\phi^2\phi^2\delta^2\delta^2)$

[a]: The SF states characterized by the total angular momentum projection $M_L = \sum m_\ell$ are denoted using the $D_\infty h$ parent symmetry. [b]: Numbers indicate the weight of the configurations in %, only contributions larger than 5% are listed.

Energies and assignment of the lowest Spin-Orbit electronic states in $Ln(COT)_2^-$

Table S7: Relative energies (cm^{-1}) and assignment (per-cent) of the SO states issued from the SO ground multiplet $^{2s+1}L_J$. CAS(n,7)SCF-SO calculations.

$^{2s+1}L_J$ Multiplet	M_J States	ΔE	Major Configurations[a]
		$Ce(COT)_2^-$	
$^2F_{5/2}$	±1/2	0	54 $^2\Sigma$, 46 $^2\Pi$
	±5/2	479	94 $^2\Phi$, 6 $^2\Delta$
	±3/2	1040	59 $^2\Pi$, 41 $^2\Delta$
		$Pr(COT)_2^-$	
$^3H_4$	±3	0	65 $^3\Gamma$, 28 $^3\Phi$, 4 $^3\Delta$, 2 $^1\Phi$
	±2	182	59 $^3\Phi$, 32 $^3\Delta$, 7 $^3\Pi$, 2 $^1\Delta$
	±1	550	41 $^3\Delta$, 16 $^3\Sigma$, 18 $^3\Pi$, 2 $^1\Pi$
	0	645	44 $^3\Sigma$, 54 $^3\Pi$, 2 $^1\Sigma$
	±4	894	6 $^3\Phi$, 37 $^3\Gamma$, 54 ^3H, 2 $^1\Gamma$
		$Nd(COT)_2^-$	
$^4I_{9/2}$	±5/2	0	37 $^4\Phi$, 44 $^4\Gamma$, 14 $^4\Delta$
	±7/2	156	12 $^4\Phi$, 36 $^4\Gamma$, 48, ^4H
	±3/2	204	38 $^4\Phi$, 38 $^4\Delta$, 18 $^4\Pi$, 4 $^4\Sigma$
	±1/2	488	24 $^4\Delta$, 46 $^4\Pi$, 27 $^4\Sigma$
	±9/2	552	7 $^4\Gamma$, 24 ^4H, 66 ^4I
		$Pm(COT)_2^-$	
$^5I_4$	±4	0	78 ^5I, 17 ^5H, 4 $^5\Gamma$
	0	42	34 $^5\Sigma$, 49 $^5\Pi$, 17 $^5\Delta$
	±1	144	22 $^5\Sigma$, 39 $^5\Pi$, 27 $^5\Delta$, 11 $^5\Phi$
	±3	339	52 ^5H, 30 $^5\Gamma$, 13 $^5\Phi$, 4 $^5\Delta$
	±2	352	31 $^5\Phi$, 27 $^5\Delta$, 23 $^5\Gamma$, 15 $^5\Pi$, 4 $^5\Sigma$
		$Sm(COT)_2^-$	
$^6H_{5/2}$	±5/2	0	81 ^6H, 14 $^6\Gamma$, 4 $^6\Phi$
	±1/2	276	42 $^6\Pi$, 26 $^6\Sigma$, 24 $^6\Delta$, 8 $^6\Phi$
	±3/2	432	25 $^6\Delta$, 25 $^6\Phi$, 22 $^6\Pi$, 17 $^6\Gamma$, 11 $^6\Sigma$
		$Eu(COT)_2^-$	
$^7F_0$	0	0	41 $^7\Delta$, 36 $^7\Phi$, $^7\Pi$, $^7\Sigma$
		$Gd(COT)_2^-$	
$^8S_{7/2}$	±7/2	0	100 $^8\Sigma$
	±5/2	73	100 $^8\Sigma$
	±3/2	121	100 $^8\Sigma$
	±1/2	146	100 $^8\Sigma$
		$Tb(COT)_2^-$	
$^7F_6$	0	0	47 $^7\Sigma$, 45 $^7\Pi$, 5 $^7\Delta$
	±1	40	46 $^7\Pi$, 40 $^7\Sigma$, 7 $^7\Delta$
	±2	161	49 $^7\Pi$, 33 $^7\Sigma$, 13 $^7\Delta$
	±3	356	49 $^7\Pi$, 26 $^7\Delta$, 16 $^7\Sigma$, 6 $^7\Phi$
	±6	473	97 $^7\Phi$
	±4	585	43 $^7\Delta$, 33 $^7\Pi$, 21 $^7\Phi$
	±5	676	59 $^7\Phi$, 38 $^7\Delta$

[a]: Only the SF ^{2s+1}L configurations larger than 5% are given.

Table S8: Relative energies (cm^{-1}) and assignment (per-cent) of the SO states issued from the SO ground multiplet ${}^{2s+1}L_J$. CAS(n,7)SCF-SO calculations.

${}^{2s+1}L_J$ Multiplet	M_J States	ΔE	Major Configurations[a]
		$Dy(COT)_2^-$	
${}^6H_{15/2}$	±9/2	0	48 ${}^6\Phi$, 24 ${}^6\Delta$, 21 ${}^6\Gamma$
	±11/2	25	49 ${}^6\Phi$, 45 ${}^6\Gamma$, 6 ${}^6H$
	±7/2	38	40 ${}^6\Delta$, 33 ${}^6\Phi$, 13 ${}^6\Pi$, 8 ${}^6\Gamma$
	±5/2	89	39 ${}^6\Delta$, 32 ${}^6\Pi$, 15 ${}^6\Phi$, 7 ${}^6\Sigma$, 2 ${}^6\Gamma$
	±3/2	128	44 ${}^6\Pi$, 24 ${}^6\Delta$, 23 ${}^6\Sigma$, 5 ${}^6\Phi$
	±1/2	149	47 ${}^6\Pi$, 38 ${}^6\Sigma$, 10 ${}^6\Delta$, 1 ${}^6\Phi$
	±13/2	206	73 ${}^6\Gamma$, 23 ${}^6H$
	±15/2	785	96 ${}^6H$
		$Ho(COT)_2^-$	
${}^5I_8$	±5	0	45 ${}^5\Gamma$, 38 ${}^5\Phi$, 11 ${}^5H$
	±4	1	46 ${}^5\Phi$, 25 ${}^5\Delta$, 21 ${}^5\Gamma$, 2 ${}^5H$
	±3	63	42 ${}^5\Delta$, 30 ${}^5\Phi$, 16 ${}^5\Pi$, 6 ${}^5\Gamma$
	±6	85	54 ${}^5\Gamma$, 36 ${}^5H$, 4 ${}^5I$
	±2	149	36 ${}^5\Delta$, 36 ${}^5\Pi$, 11 ${}^5\Phi$, 10 ${}^5\Sigma$
	±1	221	46 ${}^5\Pi$, 30 ${}^5\Sigma$, 17 ${}^5\Delta$, 2 ${}^5\Phi$
	±7	247	72 ${}^5H$, 22 ${}^5I$
	0	248	47 ${}^5\Pi$, 40 ${}^5\Sigma$, 8 ${}^5\Delta$
	±8	403	95 ${}^5I$
		$Er(COT)_2^-$	
${}^4I_{15/2}$	±15/2	0	98 ${}^4I$
	±1/2	160	48 ${}^4\Pi$, 42 ${}^4\Sigma$, 7 ${}^4\Delta$
	±13/2	165	77 ${}^4H$, 20 ${}^4I$
	±3/2	214	47 ${}^4\Pi$, 28 ${}^4\Delta$, 18 ${}^4\Sigma$, 4 ${}^4\Phi$
	±5/2	300	48 ${}^4\Delta$, 26 ${}^4\Pi$, 16 ${}^4\Phi$, 2 ${}^4\Gamma$
	±11/2	320	60 ${}^4\Gamma$, 35 ${}^4H$, 3 ${}^4I$
	±7/2	374	47 ${}^4\Phi$, 36 ${}^4\Delta$, 14 ${}^4\Gamma$
	±9/2	392	47 ${}^4\Phi$, 43 ${}^4\Gamma$, 8 ${}^4H$
		$Tm(COT)_2^-$	
${}^3H_6$	±6	0	99 ${}^3H$
	±5	501	80 ${}^3\Gamma$, 19 ${}^3H$
	0	519	55 ${}^3\Sigma$, 44 ${}^3\Pi$
	±1	536	53 ${}^3\Pi$, 32 ${}^3\Sigma$, 14 ${}^3\Delta$
	±2	576	45 ${}^3\Delta$, 42 ${}^3\Pi$, 8 ${}^3\Phi$
	±3	619	55 ${}^3\Delta$, 40 ${}^3\Phi$, 4 ${}^3\Gamma$
	±4	629	67 ${}^3\Phi$, 30 ${}^3\Gamma$, 1 ${}^3H$
		$Yb(COT)_2^-$	
${}^2F_{7/2}$	±5/2	0	86 ${}^2\Delta$, 14 ${}^2\Phi$
	±7/2	156	100 ${}^2\Phi$
	±3/2	424	69 ${}^2\Pi$, 31 ${}^2\Delta$
	±1/2	710	56 ${}^2\Sigma$, 44 ${}^2\Pi$

[a]: Only the SF ${}^{2s+1}L$ configurations larger than 5% are given.

Crystal Field Theory

The crystal field Hamiltonian for a f complex in a $\mathcal{D}_{8h}$ symmetry can be written as:

$$\hat{H}^{CF} = B_2^0 C_2^0 + B_4^0 C_4^0 + B_6^0 C_6^0 \tag{S1}$$

with

$$C_k^q(\theta, \phi) = \sqrt{\frac{4\pi}{2k+1}} Y_k^q(\theta, \phi) \tag{S2}$$

and B_k^q some coefficients that include an integral over the radial part of the wavefunctions.

If the spin-orbit coupling is relatively large compared to the crystal field interaction, the magnetic behavior of the lanthanide ion can be described by considering only the ground multiplet $^{2S+1}L_J$. This restriction to the ground multiplet has the advantage that only the matrix elements $\langle J M_J | \hat{H}^{CF} | J M_J' \rangle$ are needed for the calculation of the energies of the low energy spectrum. Due to the spherical tensor structure of the $\hat{H}^{CF}$ operator, the matrix elements $\langle J M_J | \hat{H}^{CF} | J M_J' \rangle$ are easily evaluated by application of the so-called operator equivalent technique.[13] This technique is based on the fact that CF operators $C_k^{(q)} = \sqrt{\frac{4\pi}{2k+1}} Y_k^q$, written in spatial coordinates in terms of spherical harmonics, are equivalent to the operators $\hat{J}_x$, $\hat{J}_y$, $\hat{J}_z$ of the total angular momentum apart from a factor called Stevens coefficients.[14,15] These factors $\beta(q)$ depend on the order q of the operator and on the number of f electrons in the shell and are tabulated.[16]

The Hamiltonian defined in Eq. S1 written in terms of Stevens operators becomes

$$\hat{H}^{CF} = \beta_J(2)[B_2^0 \tilde{O}_2^0] + \beta_J(4)[B_4^0 \tilde{O}_4^0] + \beta_J(6)[B_6^0 \tilde{O}_6^0] \tag{S3}$$

where the $\beta_J(k)$ are the Stevens coefficients and are obtained using the Wigner-Eckard theorem within the J-manifold.[14] The matrix elements $\langle J M_J | \tilde{O}_q^k \hat{H}^{CF} | J M_J' \rangle$ have been listed by Abragram and Bleaney,[16] Stevens[14,15] and Judd[17] for the $k = 0$ terms. The equivalent operators $\tilde{O}_k^q$ are defined as follows:[14–16]

$$\tilde{O}_2^0 = 3J_z^2 - J(J+1) \tag{S4a}$$

$$\tilde{O}_4^0 = 35J_z^4 - 30J(J+1)J_z^2 + 25J_z^2 - 6J(J+1) + 3J^2J(J+1)^2 \tag{S4b}$$

$$\begin{aligned}\tilde{O}_6^0 = {} & 231J_z^6 - 315J(J+1)J_z^4 + 735J_z^4 + 105J^2(J+1)^2J_z^2 - 525J(J+1)J_z^2 \\ & +294J_z^2 - 5J^3J(J+1)^3 + 40J^2J(J+1)^2 - 60J(J+1)\end{aligned} \tag{S4c}$$

For the linear CF, the operator matrix representation in the $|J, M_J\rangle$ basis is diagonal. The eigenvalues are therefore trivially obtained.

The n-fold degeneracy of each ground multiplet $^{2S+1}L_J$ is split under the influence of the linear crystal field and the energies of each m_J components as a function of the CF parameters b_2, b_4 and b_6 are given in Tables S9 and S10.

For brevity, we define the new crystal field parameters b_2, b_4 and b_6 as follows:

$$b_2 = \beta_J(2) \cdot F(2) \cdot B_2^0 \tag{S5a}$$
$$b_4 = \beta_J(4) \cdot F(4) \cdot B_4^0 \tag{S5b}$$
$$b_6 = \beta_J(6) \cdot F(6) \cdot B_6^0 \tag{S5c}$$

where:

$$B_2^0 = A_2^0 \cdot \langle r^2 \rangle \tag{S6a}$$
$$B_4^0 = A_4^0 \cdot \langle r^4 \rangle \tag{S6b}$$
$$B_6^0 = A_6^0 \cdot \langle r^6 \rangle \tag{S6c}$$

and the numbers $F(n)$ are multiplying factors common to all $|J, M_J\rangle$ basis. The crystal field parameters B_2^0, B_4^0 and B_6^0 are resumed in Tables S11 and S12

Table S9: Stevens coefficients β_J(n), multiplying factors $F(n)$, and energies of the m_J states of each ground multiplets $^{2S+1}L_J$.

	Stevens Coefficients $\beta_J(n)$	$F(n)$	m_J States	Energy of m_J States
$Ce(COT)_2^-$	$\beta_J(2) = -\frac{2}{35}$	$F(2) = 2$	$m_J = \pm 1/2$	$E = -4b_2 + 2b_4$
	$\beta_J(4) = \frac{2}{315}$	$F(4) = 60$	$m_J = \pm 3/2$	$E = -1b_2 - 3b_4$
			$m_J = \pm 5/2$	$E = 5b_2 + 1b_4$
$Pr(COT)_2^-$	$\beta_J(2) = -\frac{52}{2475}$	$F(2) = 1$	$m_J = 0$	$E = -20b_2 + 18b_4 - 20b_6$
	$\beta_J(4) = -\frac{4}{5445}$	$F(4) = 60$	$m_J = \pm 1$	$E = -17b_2 + 9b_4 + 1b_6$
	$\beta_J(6) = \frac{272}{4459455}$	$F(6) = 1260$	$m_J = \pm 2$	$E = -8b_2 - 11b_4 + 22b_6$
			$m_J = \pm 3$	$E = 7b_2 - 21b_4 - 17b_6$
			$m_J = \pm 4$	$E = 28b_2 + 14b_4 + 4b_6$
$Nd(COT)_2^-$	$\beta_J(2) = -\frac{7}{1089}$	$F(2) = 6$	$m_J = \pm 1/2$	$E = -4b_2 + 18b_4 - 8b_6$
	$\beta_J(4) = -\frac{136}{467181}$	$F(4) = 84$	$m_J = \pm 3/2$	$E = -3b_2 + 3b_4 + 6b_6$
	$\beta_J(6) = -\frac{1615}{42513471}$	$F(6) = 5040$	$m_J = \pm 5/2$	$E = -1b_2 - 17b_4 + 10b_6$
			$m_J = \pm 7/2$	$E = 2b_2 - 22b_4 - 11b_6$
			$m_J = \pm 9/2$	$E = 6b_2 + 18b_4 + 3b_6$
$Pm(COT)_2^-$	$\beta_J(2) = \frac{14}{1815}$	$F(2) = 1$	$m_J = 0$	$E = -20b_2 + 18b_4 - 20b_6$
	$\beta_J(4) = \frac{952}{2335905}$	$F(4) = 60$	$m_J = \pm 1$	$E = -17b_2 + 9b_4 + 1b_6$
	$\beta_J(6) = \frac{2584}{42513471}$	$F(6) = 1260$	$m_J = \pm 2$	$E = -8b_2 - 11b_4 + 22b_6$
			$m_J = \pm 3$	$E = 7b_2 - 21b_4 - 17b_6$
			$m_J = \pm 4$	$E = 28b_2 + 14b_4 + 4b_6$
$Sm(COT)_2^-$	$\beta_J(2) = \frac{13}{315}$	$F(2) = 2$	$m_J = \pm 1/2$	$E = -4b_2 + 2b_4$
	$\beta_J(4) = \frac{26}{10395}$	$F(4) = 60$	$m_J = \pm 3/2$	$E = -1b_2 - 3b_4$
			$m_J = \pm 5/2$	$E = 5b_2 + 1b_4$
$Tb(COT)_2^-$	$\beta_J(2) = -\frac{1}{99}$	$F(2) = 3$	$m_J = 0$	$E = -14b_2 + 84b_4 - 40b_6$
	$\beta_J(4) = \frac{2}{16335}$	$F(4) = 60$	$m_J = \pm 1$	$E = -13b_2 + 64b_4 - 20b_6$
	$\beta_J(6) = -\frac{1}{891891}$	$F(6) = 7560$	$m_J = \pm 2$	$E = -10b_2 + 11b_4 + 22b_6$
			$m_J = \pm 3$	$E = -5b_2 - 54b_4 + 43b_6$
			$m_J = \pm 4$	$E = 2b_2 - 96b_4 + 8b_6$
			$m_J = \pm 5$	$E = 11b_2 - 66b_4 - 55b_6$
			$m_J = \pm 6$	$E = 22b_2 + 99b_4 + 22b_6$

Table S10: Stevens coefficients β_J(n), multiplying factors $F(n)$, and energies of the m_J states of each ground multiplets $^{2S+1}L_J$.

	Stevens Coefficients $\beta_J(n)$	$F(n)$	m_J States	Energy of m_J States
$Dy(COT)_2^-$	$\beta_J(2) = -\frac{2}{315}$	$F(2) = 3$	$m_J = \pm 1/2$	$E = -21b_2 + 189b_4 - 75b_6$
	$\beta_J(4) = -\frac{8}{135135}$	$F(4) = 60$	$m_J = \pm 3/2$	$E = -19b_2 + 129b_4 - 25b_6$
	$\beta_J(6) = \frac{4}{3864861}$	$F(6) = 13860$	$m_J = \pm 5/2$	$E = -15b_2 + 23b_4 + 45b_6$
			$m_J = \pm 7/2$	$E = -9b_2 - 101b_4 + 87b_6$
			$m_J = \pm 9/2$	$E = -1b_2 - 201b_4 + 59b_6$
			$m_J = \pm 11/2$	$E = 9b_2 - 221b_4 - 39b_6$
			$m_J = \pm 13/2$	$E = 21b_2 - 91b_4 - 117b_6$
			$m_J = \pm 15/2$	$E = 35b_2 + 273b_4 + 65b_6$
$Ho(COT)_2^-$	$\beta_J(2) = -\frac{1}{450}$	$F(2) = 3$	$m_J = 0$	$E = -24b_2 + 36b_4 - 120b_6$
	$\beta_J(4) = -\frac{1}{30030}$	$F(4) = 420$	$m_J = \pm 1$	$E = -23b_2 + 31b_4 - 85b_6$
	$\beta_J(6) = -\frac{5}{3864861}$	$F(6) = 13860$	$m_J = \pm 2$	$E = -20b_2 + 17b_4 + 2b_6$
			$m_J = \pm 3$	$E = -15b_2 - 3b_4 + 93b_6$
			$m_J = \pm 4$	$E = -8b_2 - 24b_4 + 128b_6$
			$m_J = \pm 5$	$E = 1b_2 - 39b_4 + 65b_6$
			$m_J = \pm 6$	$E = 12b_2 - 39b_4 - 78b_6$
			$m_J = \pm 7$	$E = 25b_2 - 13b_4 - 169b_6$
			$m_J = \pm 8$	$E = 40b_2es + 52b_4 + 104b_6$
$Er(COT)_2^-$	$\beta_J(2) = \frac{4}{1575}$	$F(2) = 3$	$m_J = \pm 1/2$	$E = -21b_2 + 189b_4 - 75b_6$
	$\beta_J(4) = \frac{2}{45045}$	$F(4) = 60$	$m_J = \pm 3/2$	$E = -19b_2 + 129b_4 - 25b_6$
	$\beta_J(6) = \frac{8}{3864861}$	$F(6) = 13860$	$m_J = \pm 5/2$	$E = -15b_2 + 23b_4 + 45b_6$
			$m_J = \pm 7/2$	$E = -9b_2 - 101b_4 + 87b_6$
			$m_J = \pm 9/2$	$E = -1b_2 - 201b_4 + 59b_6$
			$m_J = \pm 11/2$	$E = 9b_2 - 221b_4 - 39b_6$
			$m_J = \pm 13/2$	$E = 21b_2 - 91b_4 - 117b_6$
			$m_J = \pm 15/2$	$E = 35b_2 + 273b_4 + 65b_6$
$Tm(COT)_2^-$	$\beta_J(2) = \frac{1}{99}$	$F(2) = 3$	$m_J = 0$	$E = -14b_2 + 84b_4 - 40b_6$
	$\beta_J(4) = \frac{8}{49005}$	$F(4) = 60$	$m_J = \pm 1$	$E = -13b_2 + 64b_4 - 20b_6$
	$\beta_J(6) = -\frac{5}{891891}$	$F(6) = 7560$	$m_J = \pm 2$	$E = -10b_2 + 11b_4 + 22b_6$
			$m_J = \pm 3$	$E = -5b_2 - 54b_4 + 43b_6$
			$m_J = \pm 4$	$E = 2b_2 - 96b_4 + 8b_6$
			$m_J = \pm 5$	$E = 11b_2 - 66b_4 - 55b_6$
			$m_J = \pm 6$	$E = 22b_2 + 99b_4 + 22b_6$
$Yb(COT)_2^-$	$\beta_J(2) = \frac{2}{63}$	$F(2) = 3$	$m_J = \pm 1/2$	$E = -5b_2 + 9b_4 - 5b_6$
	$\beta_J(4) = -\frac{2}{1155}$	$F(4) = 60$	$m_J = \pm 3/2$	$E = -3b_2 - 3b_4 + 9b_6$
	$\beta_J(6) = \frac{4}{27027}$	$F(6) = 1260$	$m_J = \pm 5/2$	$E = 1b_2 - 13b_4 - 5b_6$
			$m_J = \pm 7/2$	$E = 7b_2 + 7b_4 + 1b_6$

Table S11: Crystal-field parameters (cm^{-1}) obtained by a least squares fit to the SCF-SO energies.

	$Ce(COT)_2^-$	$Pr(COT)_2^-$	$Nd(COT)_2^-$	$Pm(COT)_2^-$	$Sm(COT)_2^-$
B_2^0	-282	-273	-342	-313	-443
B_4^0	-495	-477	-434	-379	-354
B_6^0		23	43	22	

Table S12: Crystal-field parameters (cm^{-1}) obtained by a least squares fit to the SCF-SO energies.

	$Tb(COT)_2^-$	$Dy(COT)_2^-$	$Ho(COT)_2^-$	$Er(COT)_2^-$	$Tm(COT)_2^-$	$Yb(COT)_2^-$
B_2^0	-494	-456	-439	-430	-420	-466
B_4^0	-273	-278	-239	-220	-194	-194
B_6^0	72	34	21	18	14	17

In both complexes, the B_2^0 and B_4^0 parameters have a large negative value while B_6^0 is much smaller in magnitude. According to Equations S3 and S4a, a negative value of B_2^0 favors a GS with large M_J value when the Stevens coefficient $\beta_J(2)$ is positive (Pm, Sm, Er, Tm and Yb). On the contrary, small M_J components are favored for negative value of the Stevens coefficient $\beta_J(2)$ (Ce, Pr, Nd, Tb, Dy and Ho). Furthermore, according to Eq. S4b, a large value of B_4^0 adds a quadratic term which favors intermediate values of M_J. In the $Ln(COT)_2^-$ series, B_2^0 increases in absolute value in the series while B_4^0 decreases. Therefore, small M_J values are characterized for the GS of $Ce(COT)_2^-$ and $Tb(COT)_2^-$, whereas large M_J values are found for $Pm(COT)_2^-$, $Sm(COT)_2^-$, $Er(COT)_2^-$ and $Tm(COT)_2^-$. Intermediate M_J values are characterized for the rest of the series (see Tables S7 and S8).

Plots of $m_\perp^L(\boldsymbol{r})$ and $m_\perp^S(\boldsymbol{r})$

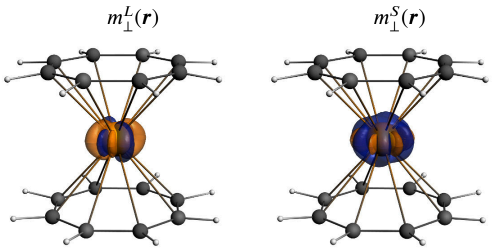

Figure S1: Orbital magnetization $m_\perp^L(\boldsymbol{r})$ and spin magnetization $m_\perp^S(\boldsymbol{r})$ density, along the $\perp$ axis for $Dy(COT)_2^-$. Isosurface values: $\pm$ 0.0001 au.

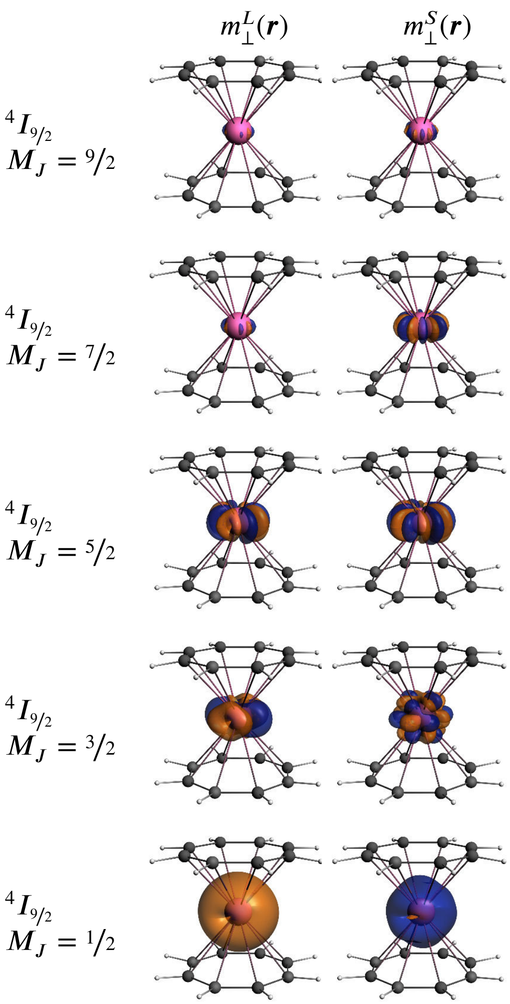

Figure S2: Orbital magnetization $m_\perp^L(\boldsymbol{r})$ and spin magnetization $m_\perp^S(\boldsymbol{r})$ density, along the $\perp$ axis for $Nd(COT)_2^-$. Isosurface values: $\pm$ 0.0001 au.

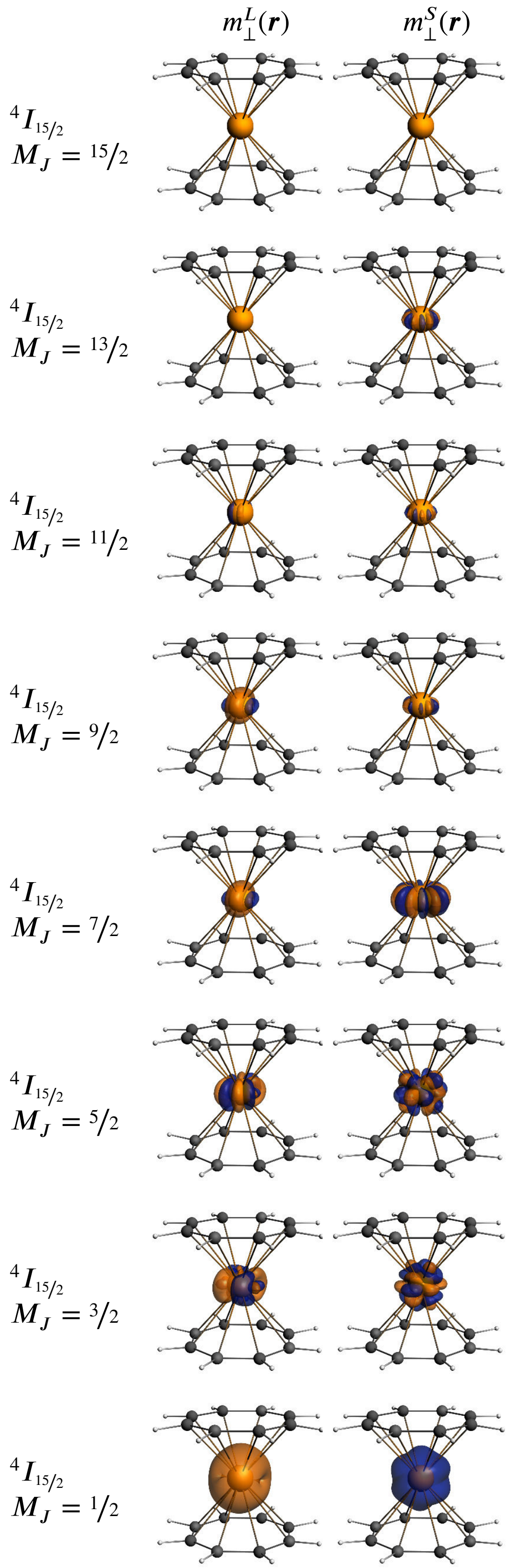

Figure S3: Orbital magnetization $m_\perp^L(\boldsymbol{r})$ and spin magnetization $m_\perp^S(\boldsymbol{r})$ density, along the $\perp$ axis for $Er(COT)_2^-$. Isosurface values: $\pm$ 0.0001 au.

Natural Orbitals of the ground states in $Ln(COT)_2^-$

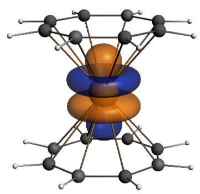

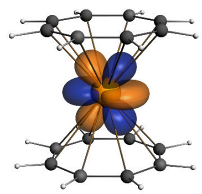

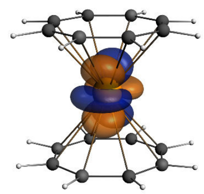

	$4f_\sigma$	$4f_{\pi_1}$	$4f_{\pi_2}$
$Ce(COT)_2^-$	0.538	0.231	0.231
$Pr(COT)_2^-$	0.262	0.368	0.368
$Nd(COT)_2^-$	0.310	0.625	0.625
$Pm(COT)_2^-$	0.809	0.586	0.586
$Sm(COT)_2^-$	0.969	0.918	0.918
$Eu(COT)_2^-$	0.943	0.914	0.914
$Gd(COT)_2^-$	1.003	1.001	1.001

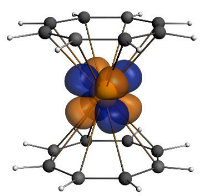

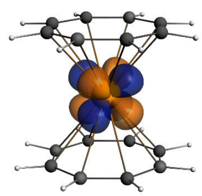

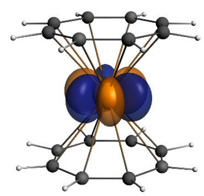

	$4f_{\delta_1}$	$4f_{\delta_2}$	$4f_{\phi_1}$
$Ce(COT)_2^-$	0.000	0.000	0.000
$Pr(COT)_2^-$	0.050	0.050	0.631
$Nd(COT)_2^-$	0.258	0.258	0.462
$Pm(COT)_2^-$	0.508	0.508	0.500
$Sm(COT)_2^-$	0.584	0.584	0.512
$Eu(COT)_2^-$	0.793	0.793	0.821
$Gd(COT)_2^-$	1.000	1.000	0.999

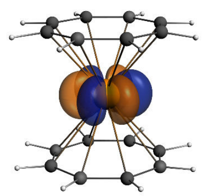

	$4f_{\phi_2}$
$Ce(COT)_2^-$	0.000
$Pr(COT)_2^-$	0.267
$Nd(COT)_2^-$	0.462
$Pm(COT)_2^-$	0.500
$Sm(COT)_2^-$	0.512
$Eu(COT)_2^-$	0.821
$Gd(COT)_2^-$	0.999

Figure S4: Selected NOs φ_p and occupation numbers n_p for $Ln(COT)_2^-$. The figure shows the NOs from the SO calculation of $Pr(COT)_2^-$. Isosurface values: ± 0.03 au.

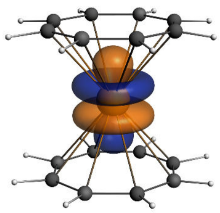 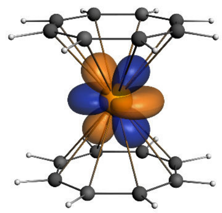 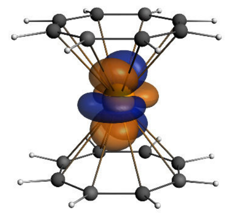

	$4f_{\sigma}$	$4f_{\pi_1}$	$4f_{\pi_2}$
$Tb(COT)_2^-$	1.478	1.234	1.234
$Dy(COT)_2^-$	1.514	1.224	1.247
$Ho(COT)_2^-$	1.380	1.550	1.550
$Er(COT)_2^-$	1.999	1.507	1.507
$Tm(COT)_2^-$	1.999	1.999	1.999
$Yb(COT)_2^-$	2.000	2.000	2.000

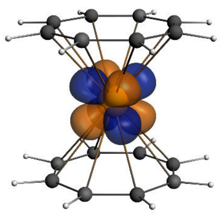 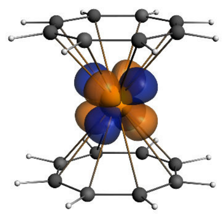 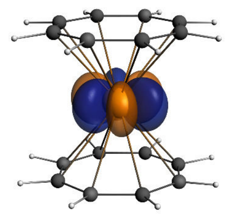

	$4f_{\delta_1}$	$4f_{\delta_2}$	$4f_{\phi_1}$
$Tb(COT)_2^-$	1.025	1.025	1.001
$Dy(COT)_2^-$	1.171	1.169	1.335
$Ho(COT)_2^-$	1.280	1.280	1.480
$Er(COT)_2^-$	1.498	1.495	1.495
$Tm(COT)_2^-$	1.503	1.503	1.497
$Yb(COT)_2^-$	1.569	1.569	1.930

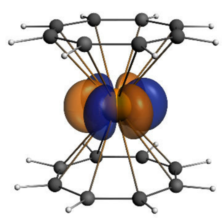

	$4f_{\phi_2}$
$Tb(COT)_2^-$	1.001
$Dy(COT)_2^-$	1.339
$Ho(COT)_2^-$	1.480
$Er(COT)_2^-$	1.495
$Tm(COT)_2^-$	1.497
$Yb(COT)_2^-$	1.930

Figure S5: Selected NOs φ_p and occupation numbers n_p for $Ln(COT)_2^-$. The figure shows the NOs from the SO calculation of $Pr(COT)_2^-$. Isosurface values: ± 0.03 au.

Natural Spin Orbitals of the ground states in $Ln(COT)_2^-$

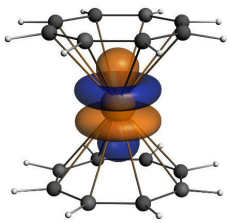 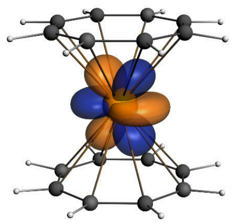 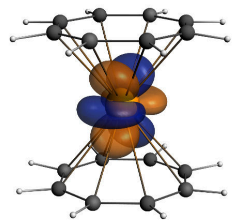

	$4f_{\sigma}$	$4f_{\pi_1}$	$4f_{\pi_2}$
$Ce(COT)_2^-$	+0.538	-0.231	-0.231
$Pr(COT)_2^-$	-0.163	+0.338	+0.338
$Nd(COT)_2^-$	+0.190	+0.254	+0.254
$Pm(COT)_2^-$	+0.781	+0.480	+0.480
$Sm(COT)_2^-$	+0.969	+0.918	+0.918
$Gd(COT)_2^-$	+0.997	+0.996	0.996

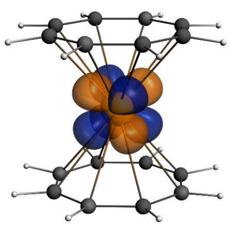 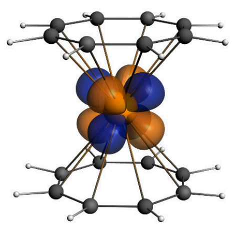 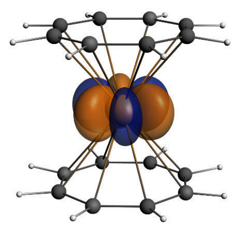

	$4f_{\delta_1}$	$4f_{\delta_2}$	$4f_{\phi_1}$
$Ce(COT)_2^-$	0.000	0.000	0.000
$Pr(COT)_2^-$	-0.031	-0.031	+0.388
$Nd(COT)_2^-$	+0.082	+0.082	+0.317
$Pm(COT)_2^-$	+0.433	+0.433	+0.433
$Sm(COT)_2^-$	+0.584	+0.584	+0.512
$Gd(COT)_2^-$	+0.999	+0.999	+0.999

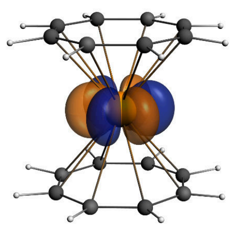

	$4f_{\phi_2}$
$Ce(COT)_2^-$	0.000
$Pr(COT)_2^-$	+0.388
$Nd(COT)_2^-$	+0.317
$Pm(COT)_2^-$	+0.433
$Sm(COT)_2^-$	+0.512
$Gd(COT)_2^-$	+0.999

Figure S6: Selected NSOs $\varphi_p^{\parallel}$ and contributions $n_p^{\parallel}$ to $m_{\parallel}^{S}(\boldsymbol{r})$ for $Ln(COT)_2^-$. The figure shows the NSOs from the SO calculation of $Pr(COT)_2^-$. Isosurface values: ± 0.03 au.

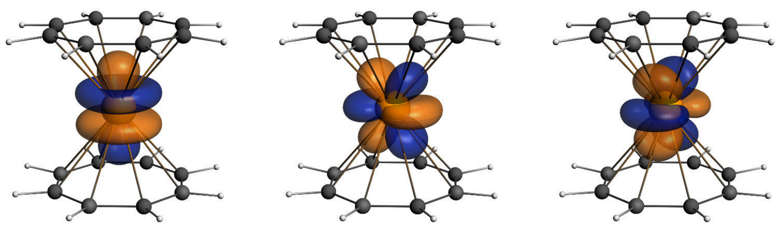

	$4f_{\sigma}$	$4f_{\pi_1}$	$4f_{\pi_2}$
$Dy(COT)_2^-$	+0.117	+0.468	+0.480
$Ho(COT)_2^-$	+0.496	+0.083	+0.083
$Er(COT)_2^-$	+0.000	+0.492	+0.492
$Tm(COT)_2^-$	+0.000	+0.000	+0.000
$Yb(COT)_2^-$	+0.000	+0.000	+0.000

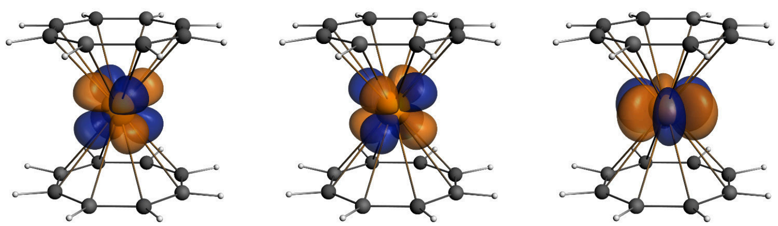

	$4f_{\delta_1}$	$4f_{\delta_2}$	$4f_{\phi_1}$
$Dy(COT)_2^-$	+0.448	+0.448	+0.494
$Ho(COT)_2^-$	+0.497	+0.497	+0.409
$Er(COT)_2^-$	+0.488	+0.488	+0.496
$Tm(COT)_2^-$	+0.497	+0.497	+0.497
$Yb(COT)_2^-$	+0.431	+0.431	-0.071

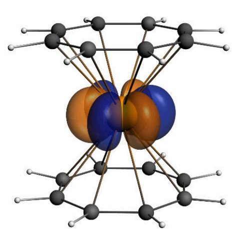

	$4f_{\phi_2}$
$Dy(COT)_2^-$	+0.494
$Ho(COT)_2^-$	+0.409
$Er(COT)_2^-$	+0.496
$Tm(COT)_2^-$	+0.497
$Yb(COT)_2^-$	-0.071

Figure S7: Selected NSOs $\varphi_p^{\parallel}$ and contributions $n_p^{\parallel}$ o $m_{\parallel}^{S}(\boldsymbol{r})$ for $Ln(COT)_2^-$. The figure shows the NSOs from the SO calculation of $Pr(COT)_2^-$. Isosurface values: $\pm$ 0.03 au.

References

[1] G. te Velde, F. M. Bickelhaupt, E. J. Baerends, S. J. A. van Gisbergen, C. Fonseca Guerra, J. G. Snijders, T. Ziegler, *J. Comput. Chem.*, 2001, **22**, 931–967.

[2] C. Fonseca Guerra, J. G. Snijders, G. Te Velde, E. J. Baerends, *Theor. Chem. Acc.*, 1998, **99**, 391.

[3] E. J. Baerends, T. Ziegler, J. Autschbach, D. Bashford, A. Bérces, F. M. Bickelhaupt, C. Bo, P. M. Boerrigter, L. Cavallo, D. P. Chong, L. Deng, R. M. Dickson, D. E. Ellis, M. van Faassen, L. Fan, T. H. Fischer, C. Fonseca Guerra, A. Ghysels, A. Giammona, S. J. A. van Gisbergen, A. W. Götz, J. A. Groeneveld, O. V. Gritsenko, M. Grüning, S. Gusarov, F. E. Harris, P. van den Hoek, C. R. Jacob, H. Jacobsen, L. Jensen, J. W. Kaminski, G. van Kessel, F. Kootstra, A. Kovalenko, M. V. Krykunov, E. van Lenthe, D. A. McCormack, A. Michalak, M. Mitoraj, J. Neugebauer, V. P. Nicu, L. Noodleman, V. P. Osinga, S. Patchkovskii, P. H. T. Philipsen, D. Post, C. C. Pye, W. Ravenek, J. I. Rodríguez, P. Ros, P. R. T. Schipper, G. Schreckenbach, J. S. Seldenthuis, M. Seth, J. G. Snijders, M. Solà, M. Swart, D. Swerhone, G. te Velde, P. Vernooijs, L. Versluis, L. Visscher, O. Visser, F. Wang, T. A. Wesolowski, E. M. van Wezenbeek, G. Wiesenekker, S. K. Wolff, T. K. Woo, A. L. Yakovlev, *Amsterdam Density Functional, SCM, Theoretical Chemistry, Vrije Universiteit, Amsterdam, The Netherlands.*, URL `http://www.scm.com`. Accessed 05/15. `http://www.scm.com`.

[4] E. van Lenthe, E. J. Baerends, J. G. Snijders, *J. Chem. Phys.*, 1993, **99**, 4597–4610.

[5] A. D. Becke, *J. Chem. Phys.*, 1993, **98**, 5648–5652.

[6] F. Aquilante, L. De Vico, N. Ferré, G. Ghigo, P. Malmqvist, P. Neogrády, T. B. Pedersen, M. Pitoňák, M. Reiher, B. O. Roos, L. Serrano-Andrés, M. Urban, V. Veryazov, R. Lindh, *J. Comput. Chem.*, 2010, **31**, 224–247.

[7] F. Gendron, D. Páez-Hernández, F.-P. Notter, B. Pritchard, H. Bolvin, J. Autschbach, *Chem. Eur. J.*, 2014, **20**, 7994–8011.

[8] F. Gendron, B. Pritchard, H. Bolvin, J. Autschbach, *Inorg. Chem.*, 2014, **53**, 8577–8592.

[9] A. Wolf, M. Reiher, B. A. Hess, *J. Chem. Phys.*, 2002, **117**, 9215–9226.

[10] P.-A. Malmqvist, B. O. Roos, B. Schimmelpfennig, *Chem. Phys. Lett.*, 2002, **357**, 230–240.

[11] H. Bolvin, *ChemPhysChem*, 2006, **7**, 1575–1589.

[12] B. Pritchard, Ph.D. thesis, University at Buffalo, State University of New York, 2014.

[13] M. T. Hutchings, *Soldi State Physics*, 1964, **16**, 227.

[14] K. W. H. Stevens, *Proc. Phys. Soc. A.*, 1952, **65**, 209.

[15] J. Elliot, K. W. H. Stevens, *Proc. Roy. Soc. A.*, 1953, **219**, 387–404.

[16] A. Abragam, B. Bleaney, *Electron paramagnetic resonance of transition ions*, Clarendon Press, Oxford, 1970.

[17] B. R. Judd, *Proc. Phys. Soc. A.*, 1955, **227**, 552.